AN ASSESSMENT OF FUNDAMENTALS OF NEUTRON POROSITY INTERPRETATION: AMERICIUM-BERYLLIUM SOURCE VERSUS NEUTRON GENERATOR-BASED ALTERNATIVES

Ahmed Badruzzaman, *Pacific Consultants and Engineers*
Andrea Schmidt, *Lawrence Livermore National Laboratory*
Arlyn Antolak, *Sandia National Laboratories*

This paper was prepared for presentation at the SPWLA 58th Annual Logging Symposium held in Oklahoma City, Oklahoma, USA, June 17-21, 2017.

ABSTRACT

Basics of ratio-based porosity response of four proposed generator-based neutron tools are studied using Monte Carlo simulation of the radiation transport to examine, at a fundamental level, their potential to replace Americium-Beryllium (Am-Be) sources. Accelerator-based sources considered include a dense plasma focus (DPF) alpha-particle accelerator, Deuterium-Tritium (D-T), Deuterium-Deuterium (D-D), and Deuterium–Lithium (D-Li7) neutron generators. The DPF alpha-particle accelerator utilizes the (α-Be) reaction generating a neutron spectrum that is nearly identical to that from an Am-Be source. D-T and D-D neutron generators utilize compact linear accelerators and emit, respectively, 14.1 and 2.45 MeV neutrons. The D-Li7 neutron spectrum resembles the Am-Be spectrum at lower energies, and has a neutron peak at 13.3 MeV.

In the present work, simple spherical geometry models that do not include tool and borehole are first used to explore the basic physics. A tool-borehole-formation configuration is then utilized to briefly explore key observations from the simpler model. In both models, the responses at various detectors are examined to understand the behavior of the ratios constructed. Sensitivity to formation conditions such as low porosity and presence of thermal absorbers, and operational conditions, such as tool standoff are examined. The state of neutron generator technology is also discussed in terms of neutron yield, target properties, power demands, etc., which would be important considerations in actually utilizing generators in nuclear logging tools.

INTRODUCTION

For over fifty years, down-hole devices using radioisotopes Cs-137 and Am-241, have been utilized, together with electrical resistivity/induction, to map the subsurface in open holes.[1] [Ellis, 1987] The 662-keV gamma rays produced by Cs-137 are utilized in 2-3 detector tools to determine the formation bulk density which then provides the most accurate measure of porosity. In an Am-Be source, alpha particles (^{4}He) emitted by Am-241 impinge on beryllium to produce a broad spectrum of source neutrons which can then be utilized to compute the neutron porosity. The neutron porosity, often in conjunction with the density, is used to determine lithology and locate gas. Recently, Am-Be (n-gamma) capture spectroscopy tools were developed to determine mineralogical information. [Herron and Herron 1996; Galford et al 2009] In addition, acoustic devices to measure porosity are often included in the suite of logging measurements. In special cases, nuclear magnetic resonance (NMR)-based techniques are also used to compute the porosity. [Ellis and Singer 2007] It should be noted that radionuclide tools are used for data acquisition both in the wireline mode where tools are inserted in the well-bore post-drilling and during logging-while-drilling (LWD).

Although well logging sources contain much lower levels of radioactivity relative to radionuclides used in other industries, such sources are small, mobile, and often utilized in unstable regions of the world, and thus pose unique safety and security risks. Despite the well-defined safety and security protocols in place to handle radionuclide logging sources, recent world events have heightened these concerns. Incidents of lost and stolen sources involving both Am-Be and Cs-137 sources and a breached Cs-137 source illustrate the underlying challenges in using such sources. [Guardian, 2003; NRC, 2006; Badruzzaman et al, 2009; Rhoades, 2010]

Consequently, enhancing security and safety of these

[1] Pu-238-based neutron porosity tools are also utilized by some operators.

sources and possibly replacing associated tools with alternative technologies to reduce the potential for vulnerability to radiological dispersal devices (RDD) have been of interest to governments and agencies for some time. The US National Academy Sciences in its 2008 report to Congress on industrial use of radioisotopes and their possible replacement suggested that the Am-Be logging source be replaced either with a D-T neutron generator or a Cf-252 source. [NAS, 2008] The NAS did not suggest replacement of the Cs-137 source used in density devices mainly for two reasons: 1) it is a lower risk-category source and 2) there appears to be no viable commercial or near-commercial alternative to it.

The petroleum industry has investigated both non-nuclear and nuclear alternatives to radionuclide-based logging tools for over three decades. Acoustic and NMR porosity tools, noted previously, have from time to time been suggested as non-nuclear alternatives to radionuclide-based porosity tools. While these techniques supply additional fluid and rock information, they cannot supply such key geological properties as lithology or mineralogy and thus are unlikely to be replacements for radionuclide-based porosity tools.

Tools and interpretation algorithms using nuclear-based electronic sources (radiation generators) have been tested or marketed for both density and neutron porosity tools and, more recently, for (n-gamma) spectroscopy. Two photon-based alternatives to Cs-137 gamma-ray density concepts have been tested. One method utilized X-ray photons generated by a linear electron accelerator (Linac) to successfully field-test an actual density logging tool that, however, was not commercialized. [King et al 1987]

The other non-radionuclide density concept, first developed for cased-hole applications as a density indicator and denoted as inelastic n-gamma density (INGD), utilizes gamma rays that are produced from inelastic interaction of high-energy neutrons from a D-T source. [Wilson 1995; Badruzzaman 1998; Odom, 1999; Neuman 1999]. An LWD neutron tool using this concept was first reported in 2000 and commercialized in 2012. [Evans et al 2000; Reichel et al 2012] The drawback of this method is that the results are not always sufficiently accurate, due to the complex mix of neutron and photon physics involved. [Badruzzaman 2014]

Tested alternatives to Am-Be (or Pu-Be) neutron porosity devices include a Cf-252 LWD tool (Valant-Spaight at al 2006) and two D-T neutron generator-based tools, one for wireline logging (Mills et al, 1988; Flanagan et al, 1991) and the other for LWD (Evans et al, 2000). The Cf-252 tool exhibited a porosity that was comparable to that from an Am-Be tool. The LWD D-T tool, like the Am-Be tool, utilizes the ratio of *total* neutron counts at two detection locations, to compute the porosity and has performed reasonably well.

The deployed wireline D-T neutron porosity tool utilizes the Near/Far ratio of the *epithermal* neutron counts. Its stated advantages are that it is not impacted by absorbers, is a direct measure of the hydrogen index, and has a greater depth-of-investigation. However, its field performance has not been consistent. [Badruzzaman 2005] **Appendix A** discusses an example from the cited reference. The effect seen was likely due to a variable standoff which appears to impact the epithermal counts more.

Scott et al (1994) had reported a standoff-correction technique utilizing the relationship of the neutron slowing-down time (SDT) to the standoff. This correction technique was further enhanced to address the issue of possible variable standoff noted in the previous paragraph. [Fricke et al 2008] However, the jury is still out on the adequacy of the algorithm since the technique as utilized in the tool still starts with epithermal counts.

Recently, two D-T generator-based (n-gamma) spectral tools were reported as alternatives to Am-Be-based capture spectroscopy tools. [Pemper et al 2006; Radtke et al 2012] These tools record both inelastic gamma rays from interaction of high energy neutrons and gamma rays from thermal neutron capture, thereby providing a more complete mineralogical characterization than do the Am-Be based (n-gamma) capture spectroscopy tools noted previously. Consequently, it appears that D-T based (n-gamma) tools will likely replace Am-Be source (n-gamma) spectral tools. In this paper, we will point out the potential for performing such measurements with the other neutron generators being considered, but this will not be discussed in detail.

The general basic porosity sensitivity of D-T and Cf-252 neutrons to liquid-filled reservoirs was reported by Xu et al (2010) for an LWD tool and that of D-D source neutrons was reported by Chen et al (2012). As with the Valant-Spaight paper (2006) cited previously, Cf-252 tool of Xu et al exhibited a porosity-sensitivity similar to that of Am-Be tools (in fact it was a bit greater). The D-D concept exhibited significantly greater (ratio) porosity sensitivity versus all other neutron tools considered.

The present paper explores the response behavior of D-T and D-D neutrons in greater depth and also studies the response of D-Li7 neutrons. Since the neutron spectrum from the (α-Be) DPF generator is almost identical to that from an Am-Be source, we will limit the discussion of this source. Initially, the basics of the porosity response in the absence of the tool and borehole will be evaluated using a spherical model. We then study a full tool-borehole-formation configuration.

NEUTRON SOURCE SPECTRA

The energy spectrum of neutrons is the key determinant of the porosity sensitivity. In this section, the energy distribution of neutrons emitted by the four generators, DPF, D-T, D-D, and D-Li7 are compared.

The dense plasma focus (DPF) neutron generator accelerates a beam of helium ions onto a solid beryllium (Be) target and produces a neutron spectrum almost identical to that from an Am-Be source (see **Figure 1**).

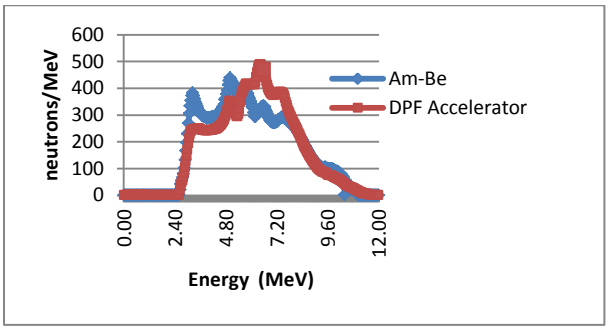

Figure 1. Am-Be vs. DPF accelerator neutron spectra from theory [Schmidt *et al* 2012]

.

Theoretical calculations indicate that the neutron yield from the DPF generator would of the same order of magnitude as that from the Am-Be source used in well logging.[2] Thus, the sensitivity to porosity is expected to be very similar.

Figure 2 displays the neutron distribution from D-T, D-D, and D-Li7 generators compared to a typical Am-Be spectrum. The D-T and D-D neutron generators emit neutrons at approximately 14.1 MeV and 2.45 MeV, respectively. The D-Li7 reaction produces a neutron distribution that is generally similar to that from an Am-Be source plus a neutron peak at 13.3 MeV. This nuclear reaction also produces gamma rays at higher discrete energies.

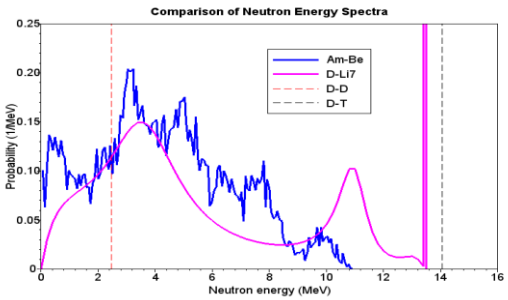

Figure 2. Neutron spectrum from ^{7}Li(d,n)^{9}Be, D-D, D-T, and ^{241}Am-Be. (Plot Courtesy of Matt Coventry of Starfire Industries using available data, Aug 30, 2015). The data for D-D and D-T reactions is from Bosch & Hale, Nucl. Fusion v32 (1992) p611-631.

We discuss the key properties of the generators later in this paper. We will see that neutron yields differ considerably across these generators. The source neutron yield determines the statistical quality of the data and hence the logging-speed of a tool.

MONTE CARLO MODELING

We performed the simulation using the Los Alamos Monte Carlo Code, MCNP, Version 5, in the analog mode (i.e., no variance reduction was used). [LANL 2003/2008]. In the spherical model, histories were run to achieve a statistical error of less than 0.5% at the farthest detector location. In the tool-borehole-formation configuration, 5% statistical error in the farthest detector was achieved.

Although the neutron yield varies across generators, in the modeling we assume a unit source for each tool model. Thus, we are assuming the same neutron yield for all generators. This will allow us to study the response characteristics with the statistical error being on the same basis. Later in the paper we will discuss the effect of differing neutron yields.

RESPONSE CHARACTERISTICS: SPHERICAL MODEL

Porosity Response: The basic porosity response of a formation is first examined without the presence of tool or borehole. We assume a sphere with the source at its center. The formation is of SiO_2 with matrix density of 2.65 g/cc. We vary the liquid-filled porosity and compute the neutron flux at radially outward cells. **Figure 3** displays the near/far (N/F) ratio of the total flux.

[2] Theoretical calculations also predict that D-D, and D-Li7 neutron generators can produce the same (or greater) yield as Am-Be. Engineering and power constraints have limited the actual yield that can be attained in a well logging tool.

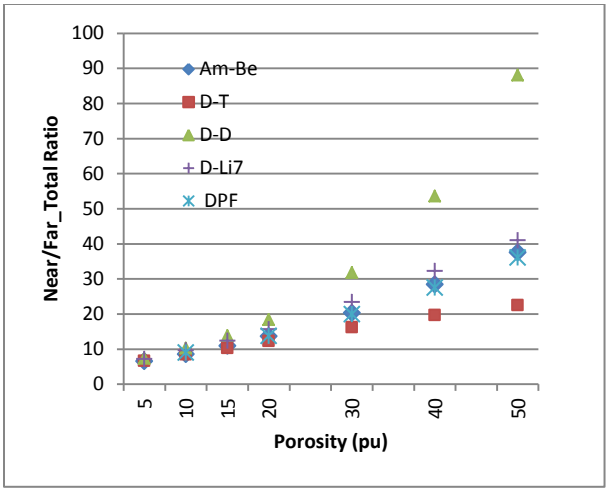

Figure 3 Spherical Model: Near/Far Ratio with D-T, D-D, D-Li7 and α-Be (DPF) versus an Am-Be source. Near and Far locations are respectively 10 inches and 22 inches from the source

We note the following:

- The α-Be (DPF) Near/Far ratio is almost identical to that from Am-Be source neutrons. This is not surprising since the spectra are nearly identical.
- The D-Li7 Near/Far ratio is similar to that from the Am-Be source, but is not identical. This reflects the similarity in their respective spectrum. We will see later that, at low porosity, the ratio does exhibit a noticeable difference versus Am-Be neutrons.
- The D-D Near/Far ratio becomes more sensitive to porosity change as the porosity increases. This confirms previous results of Chen et al (2012). We will examine this in more detail later in the paper.
- The D-T Near/Far ratio is the least sensitive to porosity as was reported previously for an LWD tool model by Xu et al (2010.)

Because of the nearly identical neutron source spectra, we will not discuss further the response characteristics of neutrons from the α-Be (DPF) neutron generator, but will comment on available operational and design issues that may arise in using this generator in well logging.

Near/Far Ratios and Fluxes: **Figure 3** depicts the ratio of total counts (sum of epithermal and thermal flux) in the near and far detectors. Neutron tools can record both total and epithermal counts. Thus, one can construct ratios of total counts and epithermal counts and relate them to porosity. Most neutron tools, including the D-T generator-based LWD tool, utilize the ratio of total counts. The marketed D-T generator-based wireline tool utilizes the N/F ratio of epithermal counts.

Figure 4 displays the thermal, total, and epithermal flux ratios. We note from the figure that the ratio of total flux generally exhibits the same shape versus porosity as that exhibited by the thermal flux ratio (for the four sources considered). This is perhaps the reason the neutron porosity obtained using the N/F ratio of total counts of neutron tools is often denoted as the *thermal neutron porosity*, even though it is not based solely on thermal counts.

We also note from **Figure 3** and **Figure 4** that the Near/Far ratio of total counts utilizing the D-D source exhibited significantly greater porosity sensitivity than those by the other sources. As seen from **Figure 5**, this arises from the much more rapid decline of (D-D-origin) flux at the Far location.

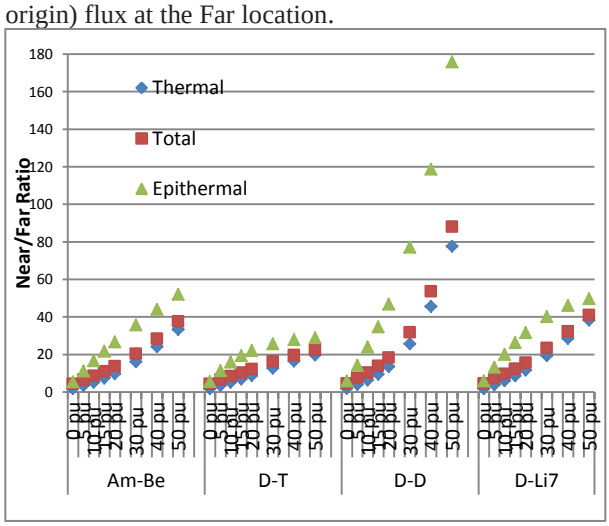

Figure 4. Near/Far ratios of Total, Epithermal and Thermal Fluxes**.** Near and Far locations are respectively 10 inches and 22 inches from the source

It was noted elsewhere that the commercial D-T wireline tool utilizes the Near/Far ratio of epithermal counts to obtain the porosity. From **Figure 4** we note that the epithermal counts ratio depicts a different behavior from either the total or thermal counts ratio and this differs across the four sources. We note the following:

- For Am-Be source neutrons, epithermal counts ratio increases with porosity only at a modest rate before becoming nearly constant at higher porosity. This can be seen in the epithermal flux displayed in **Figure 6.**

- For D-D source neutrons, all three ratios (thermal, epithermal, and total) increase with porosity, with the epithermal ratio increasing most rapidly. As discussed above, this arises from the very rapid decline in epithermal flux at the far detector location as seen in **Figure 6**. For both D-T and D-Li7 source neutrons, the epithermal Near/Far ratio initially increases with porosity at a noticeably greater rate. The rate of increase then declines as the porosity increases further. This arises from a slower rate of change in the far location epithermal flux for neutrons from these sources. Thus, especially for D-T source neutrons, the porosity response characteristics of epithermal ratio would be different from those of the total (or thermal) flux ratio. This in turn will result in a different behavior in non-nominal conditions such as low porosity, presence of thermal absorbers, or standoff.

Note that D-T and D-Li7 sources emit high-energy neutrons at 14.1 MeV and 13.3 MeV, respectively. These high-energy neutrons are able to reach the far location more than neutrons from the lower energy sources. Neutrons from lower-energy sources (like a D-D generator) are more readily thermalized in the vicinity of the generator and, consequently, are absorbed in the formation before reaching the far detector.

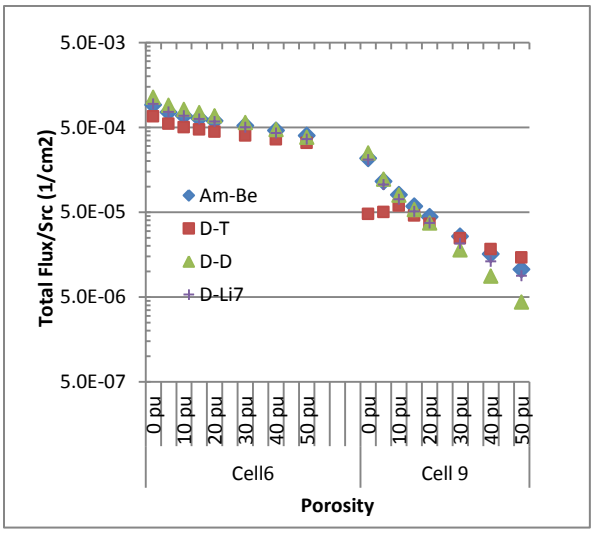

Figure 5. Total flux at near and far locations, which are the midpoints of cells, respectively, at 10 inches and 22 inches from the source.

In order to increase the neutron counts in the far detector, it can be moved closer to the generator. However, that would reduce the Near/Far ratio sensitivity and reduce the depth-of-investigation of the detector. Thus, while D-D neutrons offer the potential for greater porosity sensitivity, the much lower flux (and hence counts) at the far detector will result in a greater statistical uncertainty. This in turn would likely require a slower logging speed, even if the neutron yield from the source is identical (as we have assumed in our simulation). On the other hand, the highest flux at the far location comes from D-T neutrons. This reduces the porosity sensitivity, but would likely yield a lower statistical uncertainty and possibly allow a faster logging speed.

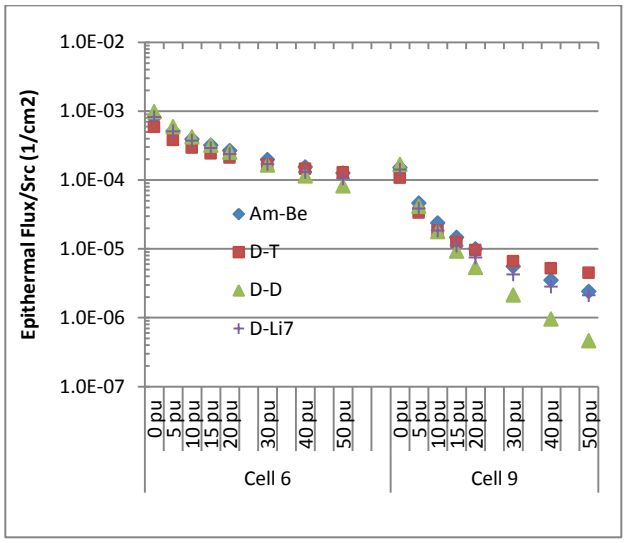

Figure 6. Epithermal flux at near and far locations, which at, respectively, 10 inches and 22 inches from the source.

Slowing Down, Diffusion, and Migration Lengths: The Near/Far ratio behavior and hence the porosity response can be understood by considering the three processes that the neutron population undergoes, namely, slowing down of energetic neutrons, the diffusion of neutrons that have slowed down to thermal energies, and their absorption. In field applications, each of these processes is affected differently by changes in formation or well-bore conditions. The behavior of these features for each source type can be related to three parameters, namely, slowing down length (L_s), diffusion length (L_d), and the macroscopic thermal absorption cross-section which is traditionally known in well-logging applications as Sigma (Σ). The slowing down length and the diffusion length can be combined, as shown in Eq. (B-2), to define a parameter denoted as the migration length, L_m. In **Appendix B**, we show a simple approach for obtaining these parameters from the fluxes computed at two different locations. Here we expand on their physical meaning.

The slowing down length, L_s, represents the average of root-mean-square distance that energetic neutrons travel

before they are thermalized. Since hydrogen is the most effective element in slowing down neutrons, the parameter reflects the impact of the hydrogen index which would increase as the pore space gets filled with hydrogenous liquids such as water or oil. The diffusion length, L_d, reflects a similar distance scale that thermal neutrons travel as they diffuse and then get absorbed. Thus, L_d is related to two parameters, the thermal diffusion coefficient (D_{th}) and Sigma (Σ), as shown in Eq. (B-3). The diffusion length decreases if the diffusion coefficient decreases as would happen with the increase in liquid-filled porosity or if Σ increases. The increase in Σ may happen for two key reasons: 1) the increasing absorption from hydrogen as the liquid-filled porosity increases or 2) the presence of thermal absorbers in the formation such as chlorine in the form of NaCl in saline water or presence of a neutron absorber such as Gadolinium in the rock.

The migration length, L_m, collectively reflects the 'travel' of a neutron population encompassing first their slowing down phase and then the thermal phase as they diffuse and get absorbed.

Using the procedure in **Appendix B**, both L_s and L_m can be computed by utilizing the epithermal Near/Far ratio and the total Near/Far ratio, respectively.

Figure 7 displays the slowing down length versus porosity computed using the epithermal ratios in **Figure 4** in Eq. (B-1). The figure shows that D-T source neutrons have the longest slowing length and D-D neutrons, as expected, have the shortest slowing length. From **Figure 2,** we noted that the energy distributions of Am-Be neutrons and D-Li7 neutrons were similar. So their slowing down lengths at higher porosities is similar.

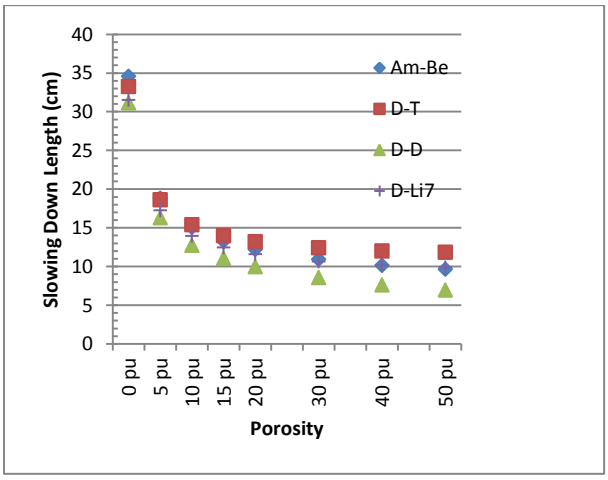

Figure 7. Slowing down length Vs. porosity in water-filled SiO_2 formation

Using the Near/Far ratio of total flux in **Figure 3** and the analog of Eq. (B-1) for L_m, we obtain the migration length displayed in **Figure 8**.

Note that D-T neutrons generally have the longest migration length at a given porosity while D-D neutrons have the shortest migration length. We also note that in the conditions studied in **Figure 3**, the slowing down length (**Figure 7**) shows a greater difference across sources than the migration length (**Figure 8**).

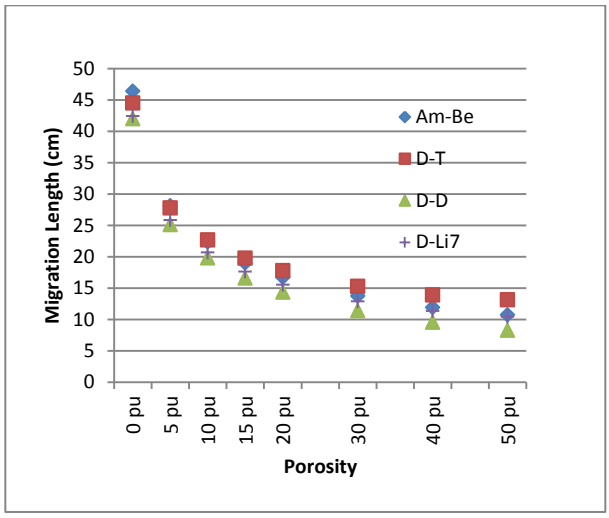

Figure 8. Migration length vs. Total flux ratio porosity in water-filled SiO_2 formation

Knowing L_s and L_m, one can compute the diffusion length, L_d using Eq. (B-2). **Figure 9** displays the diffusion length for the cases studied above.

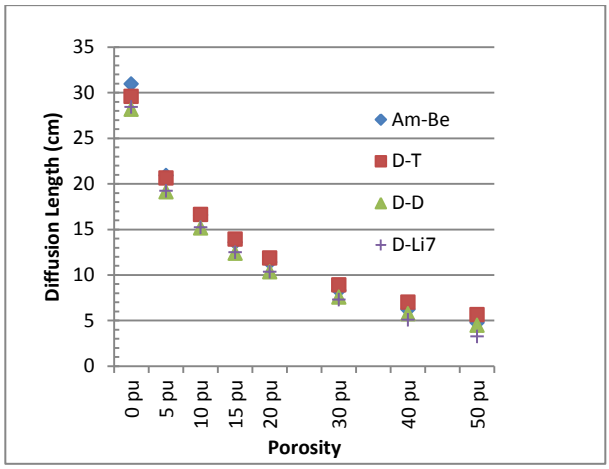

Figure 9. Diffusion length vs. porosity in a freshwater-filled SiO_2 formation.

Note that the values are practically indistinguishable, although L_d of the D-T source neutrons appears to be

the highest. As discussed previously, the decrease in L_d with porosity comes from the decrease in the thermal diffusion coefficient, D_{Th}, and the increase in Sigma.

Porosity Interpretation: The measured counts can be used to construct the Near/Far ratio which can then be used to estimate the porosity. Epithermal Near/Far ratios would give what is called the "epithermal neutron porosity." The Near/Far ratio of total counts, as noted previously, is referred to as "thermal neutron porosity." In this paper, we will denote the latter as the "total ratio porosity" to avoid confusion.

The slowing down length L_s and migration length, L_m, can also be used to obtain the epithermal and total-ratio porosities. In fact, in one of the early-generation porosity interpretation algorithms, the Near/Far ratio of measured counts was related to the appropriate length parameter calibrated to the porosity for a given lithology. [Ellis 1987] The measured epithermal Near/Far ratio would be used to compute the slowing down length which then would be used to read off the porosity for a given lithology from the calibration chart. The total Near/Far ratio can similarly be used to obtain the migration length and then the total-ratio porosity in a given lithology.

From the above discussion, it is clear that the epithermal flux will be more sensitive to changes in the hydrogen index which governs the slowing down process. Interpreting the porosity using neutrons from a given source depends on a number of factors including the dynamic range versus porosity sensitivity of the Near/Far counts ratio or L_s and L_m of neutrons from that source.

Low Porosity: Usual neutron porosity tools are not particularly sensitive to changes at low porosity (below 10-12 pu). We noted that, in general, the ratio of fluxes of neutrons from a D-D source exhibit a greater porosity sensitivity. We further examine this at low porosity to see if these neutrons offer any advantage.

Figure 10 displays the Near/Far ratio total flux in the 0-15 pu range.

It can be seen in the figure that the Near/Far ratio for Am-Be and D-T sources are essentially identical in this range. The ratio for D-D and D-Li7 neutrons is more sensitive and indicates a separation from Am-Be and D-T neutrons, especially above 5 pu.

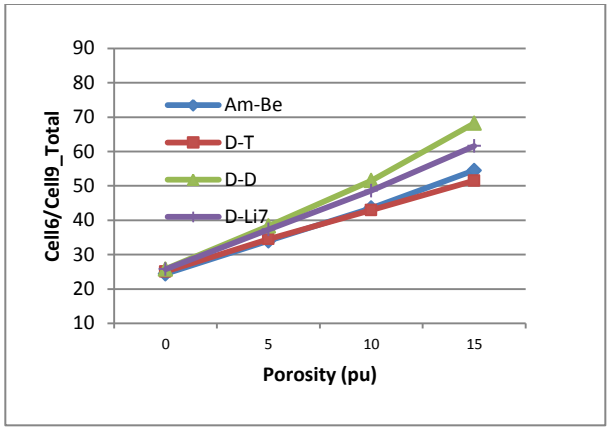

Figure 10. Near/Far ratio total flux at low porosity

Figure 11 displays the epithermal Near/Far ratio in the 0-15 pu range. The D-D and D-Li7 values of this ratio exhibit an even greater separation from the ratio of Am-Be or D-T neutrons.

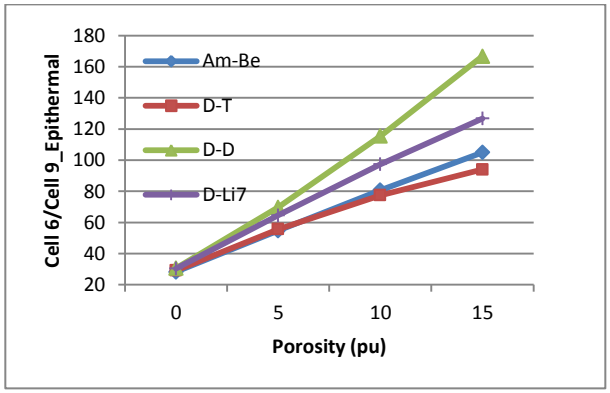

Figure 11. Near/Far ratio of epithermal flux at low porosity.

Figure 12 combines the results shown in **Figures 10** and **11** by computing the ratio of the two ratios, namely the epithermal Near/Far ratio to the total Near/Far ratio.

From **Figure 12,** we note that the ratio-of-ratios of D-D and D-Li7 neutrons has greater sensitivity compared to that of Am-Be and D-T neutrons. The implication is that one can possibly obtain a measurable porosity change in the low porosity range using D-D or D-Li7 neutrons.

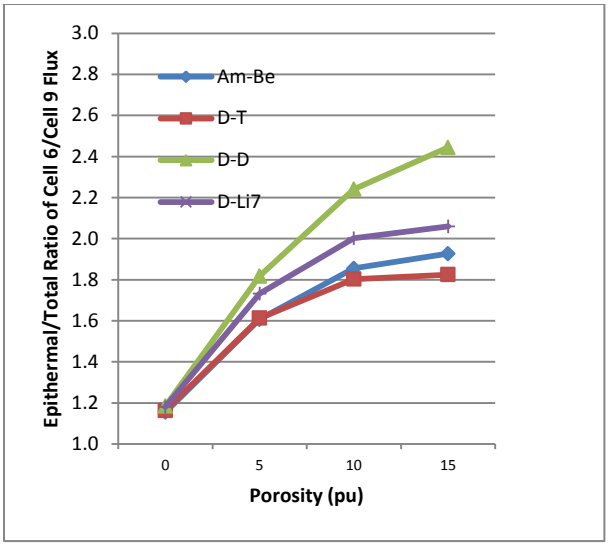

Figure 12. Ratio of ratios: epithermal flux ratio to total flux ratio.

Strong Absorbers: The effect of strong thermal absorbers on the response is analyzed by changing the salinity of the formation fluid at 30 pu; chlorine is a strong thermal neutron absorber. **Figure 13** displays the Near/Far ratios for each neutron source as the salinity varies from 0 kppm to 260 kppm.

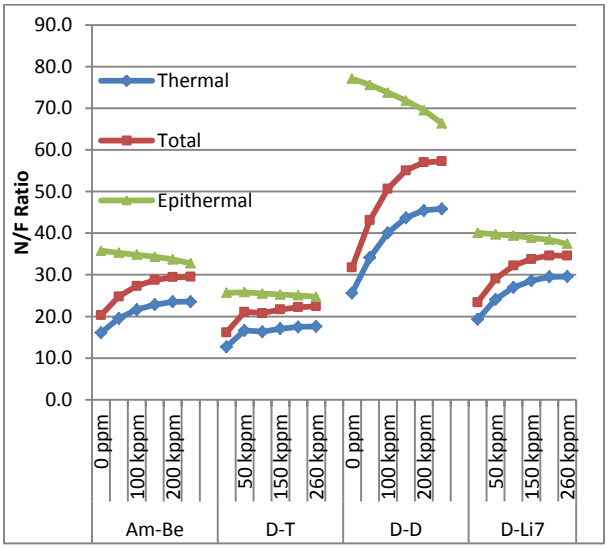

Figure 13. Near/Far total, epithermal, and thermal flux ratio of a 30-pu SiO_2 formation as the salinity varies

From the figure we note the following:

- D-D neutrons exhibit the greatest sensitivity to the salinity increase and D-T neutrons the least. This is not surprising since D-D neutrons start out at much lower energies than do D-T neutrons.
- The thermal neutron fraction would be larger with the D-D source, especially at the Far detector location.
- The thermal N/F ratio increases for all sources with the largest rate of increase being for the D-D neutron source.
- The total flux Near/Far ratio and the epithermal flux Near/Far ratio increase for all sources with D-T neutrons showing the least sensitivity and D-D neutrons the most sensitivity.
- D-Li7 neutrons exhibit a somewhat greater sensitivity than Am-Be.

We can gain some insight on the behavior of the Near/Far ratios by constructing L_s, L_m, and L_d for the conditions depicted in **Figure 13**. These are displayed in **Figure 14.** The slowing down length (L_s) shows a small but noticeable increase, especially at high salinity. This increase arises from the salt (NaCl) replacing more water in the pore space as the salinity increases, thereby reducing the hydrogen concentration and resulting in the neutrons being able to travel a longer root-mean-square distance. However, this is not sufficient to compensate for the effect of the much greater reduction in diffusion length resulting from the large increase in Sigma due to the increase in salinity.

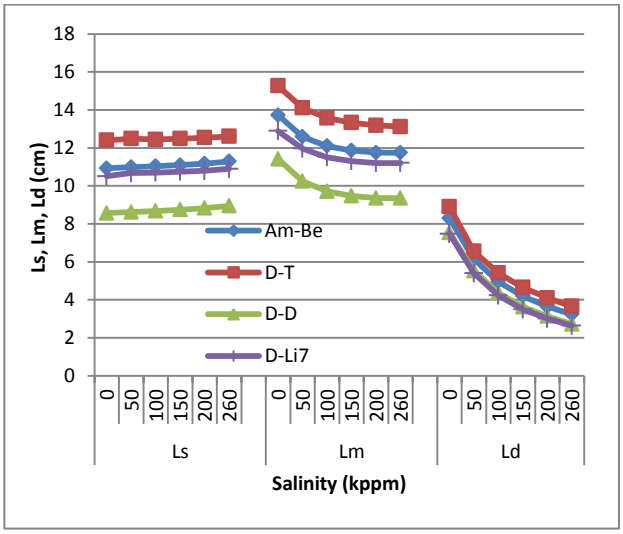

Figure 14. Slowing down, migration and diffusion length vs. salinity in a 30-pu SiO_2 formation.

The apparent porosity can be computed by referencing the data to a calibration condition. We utilize the zero-salinity formation conditions of **Figure 3** and **4** as the calibration condition. Thus, the greater sensitivity of D-D neutrons to salinity exhibited in **Figure 13** translating

into significantly different apparent porosity depends on the magnitude of the change in the Near/Far ratios due to salinity relative to the change in Near/Far ratios due to the porosity change (i.e., the calibration condition.) Using the data in **Figure 3** for each source type as its calibration, the apparent porosity is computed and displayed in **Figure 15.** From the figure we note the following:

- For neutrons from all four sources, the apparent (i.e., predicted) neutron porosity would be higher than the nominal zero-salinity porosity (30 pu). The difference is large and the increase is fastest between zero salinity and 50 kppm with the rate of increase declining with increasing salinity.

- This apparent porosity increases primarily due to the large increase in the Sigma reducing the diffusion length significantly as predicted by Eq. (B-3) and displayed in **Figure 14**. This in turn reduces the migration length (also shown in **Figure 14** relative to that in **Figure 8** for the 30-pu calibration condition and results in increasing the predicted porosity.

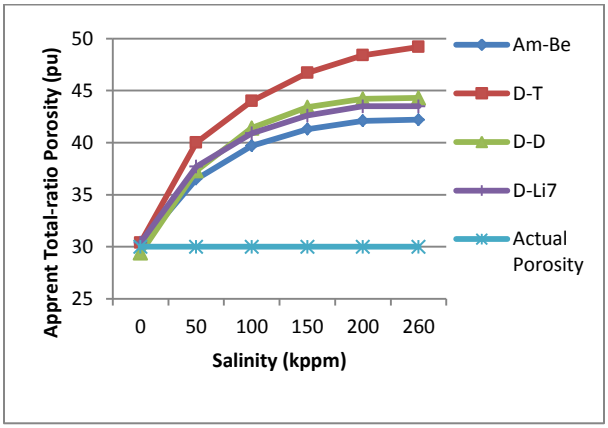

Figure 15. Apparent neutron porosity of a 30-pu SiO2 formation as the salinity increases. The reference case in **Figure 3** was used as the 'calibration.'

- Despite the total Near/Far ratio (or the migration length) of D-T neutrons showing the lowest sensitivity to salinity increase, these neutrons exhibit a higher apparent porosity versus neutrons from the other sources. This is because the zero-salinity Near/Far ratio versus. porosity (**Figure 3**) was utilized as the calibration. The latter has a smaller change in the Near/Far ratio as the porosity increases, especially at higher porosities; the change for D-T neutrons is the least. The change in the total flux Near/Far ratio due to increase in salinity is larger and, hence, the computed (apparent) porosity is higher

RESPONSE CHARACTERISTICS: A TOOL-BOREHOLE-FORMATION CONFIGUARTION

We assume a 4-detector system as displayed in **Figure 16**. We denote this as the full geometry model.

Reference Condition: We first study the configuration in **Figure 16** assuming a fresh-water filled SiO_2 formation ranging from 0 pu to 50 pu. In **Figure 16**, the tool's outer diameter is 3-5/8 inches with four He-3 detectors (in blue), respectively, at 4-inch, 10-inch, 16-inch and 26-inch locations from the source.

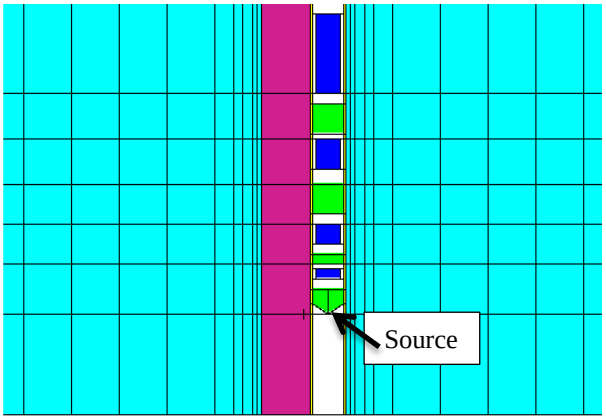

Figure 16: MCNP geometry of a four-detector model tool in an 8-3/4 inch bit freshwater borehole with no tool standoff.

Figure 17 displays the ratio of total counts in Detector 2 to that in Detector 4 (Det 2/Det 4 ratio).

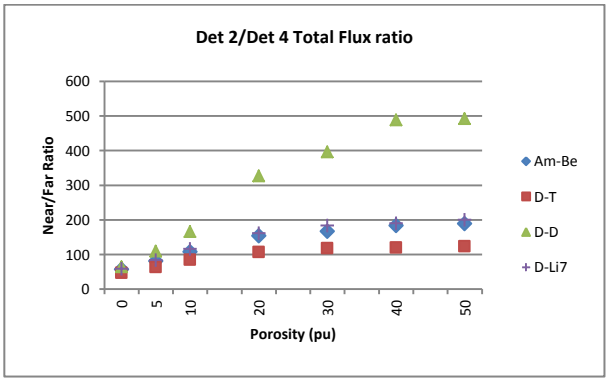

Figure 17. Ratio of total counts in Detector 2 to that in Detector 4 in the tool-borehole-formation configuration in **Figure 16**.

Figure 18 displays the Det 3/Det 4 ratio of total counts. In both figures, the results are for the total Near/Far ratio and, thus, they can be related to porosity.

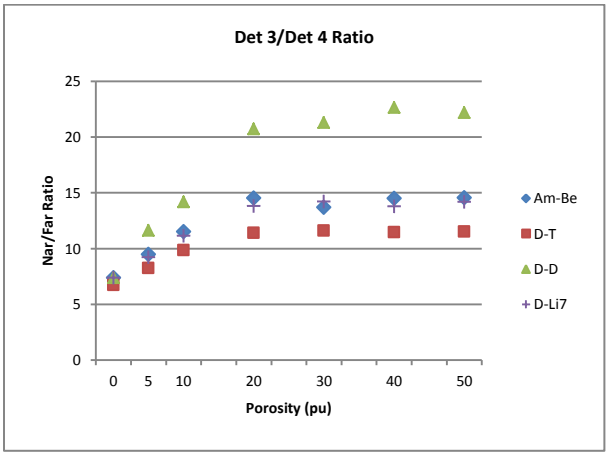

Figure 18. Ratio of total counts in detector 3 to that in detector 4 in the tool-borehole-formation configuration in **Figure 16**

We note the following from the two figures.

- As we had seen in the spherical model for neutrons from all four sources, both Near/Far ratios increase with (the liquid-filled) porosity in the full geometry model.

- The increase in porosity sensitivity is largest for D-D neutrons and smallest for D-T neutrons. The response of Am-Be and D-Li neutrons appear similar.

In order to get a better insight into the Near/Far ratios, **Figure 19** displays the response at three of the detectors.

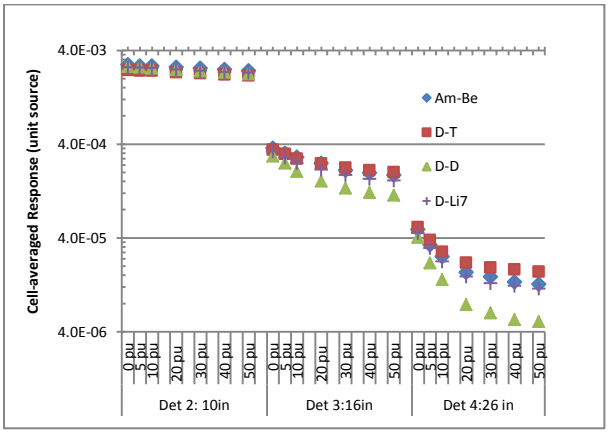

Figure 19. Counts in detectors 2, 3 and 4 in the tool-borehole-formation configuration in **Figure 16**

We note the following from the **Figure 19**.

- For all four sources, the response changes more rapidly as the detector spacing increases.

- Detector 2 (Det 2), which is at 10 inches is almost unresponsive to porosity change. Thus, the increase in the Det 2/Det 4 ratio is almost entirely due the decline in counts of the Far detector (located at 26 inches) in the current model.

- The counts decrease in Detector 3 but less so than in Detector 4. Thus, the Det 3/Det 4 ratio increases, but its magnitude in much smaller than the Det 2/Det4 ratio.

- Of the neutrons from the four sources, the decline in counts is most rapid for D-D neutrons. This results in the more rapid increase in the Near/Far ratios previously seen in **Figure 17** and **18** for D-D neutrons compared to those from the other sources.

- The least rapid decline in counts with D-T neutrons results in the Near/Far ratios for these neutrons as seen in **Figure 17** and **18.**

The Near/Far ratios in the full geometry model indicates that D-D neutrons will be the most sensitive to porosity change and would possibly be the best neutron source to utilize in determining the neutron porosity. However, the rapid decline in the counts at the farthest detector (seen to be more so in the full geometry model) to achieve this poses a challenge. Detector counts determine the statistical error and hence the logging speed for an assumed unit source. Clearly, the logging speed with a D-D source tool will be lower compared to tools with any of the other three sources, even if all sources have the same neutron yield. D-T neutrons would offer the most advantage in terms of logging speed.

The next sub-section considers the low-porosity condition that was previously investigated with the spherical model. The effect of tool standoff that was difficult to study with the spherical model is also studied.

Low Porosity: Following the procedure used in the spherical model, we constructed the ratio-of-ratios (ratio of epithermal Near/Far ratio to total Near/Far ratio) for the configuration in **Figure 16**. The results are displayed in **Figure 20**. From the figure, we note the ratio-of-ratios for D-D source neutrons indicates greater sensitivity than neutrons from the other sources

in the low porosity range. On the other hand, the effect appears to be smaller than that from the spherical model. This is likely due to the presence of the bore-hole (water-filled in this case). Presence of the water in the borehole would affect the energy and, hence, the counts to reduce the sensitivity.

Both spherical model and full geometry model analyses indicate that it *may* be possible to construct ratios using the response of D-D source tools to obtain a clearer porosity interpretation at low porosities than is currently possible. However, whether this is actually realizable in real field conditions needs a larger study; this is beyond the scope of this paper.

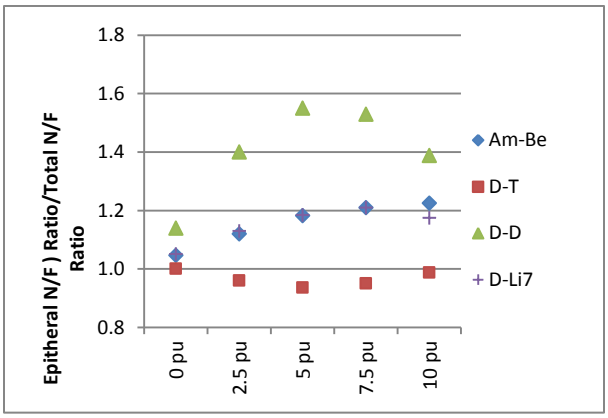

Figure 20. Ratio of two ratios, epithermal near/far ratio to total near/far ratio in 0-10 pu range for the configuration in Figure 16.

Standoff Effect: An example of the adverse effect of variable stand-off on the response of the commercial D-T generator wireline neutron porosity tool was previously noted in the paper. In order to assess how the effect may vary across the sources under consideration, the Monte Carlo simulation of the tool-borehole-formation configuration in **Figure 16** was repeated by introducing increasingly thicker standoff. The sensitivity to water standoff values of 1/8 inch, ¼ inch, ½ inch and ¾ inch, respectively, was evaluated for two formation conditions, 0 pu and 30 pu.

Figure 21 shows the variation in the size of the standoff as it increases from 1/8 inch to ¾ inch. Clearly, the amount of water the tool 'sees' will increase as the standoff increases, resulting in a higher effective liquid-filled porosity. However, two questions arise: 1) Will the effect continue to increase linearly, reduce, or even stop because the spectrum of the neutrons reaching the detectors from the formation would not change anymore, and 2) would the effect be the same across porosities, i.e., is there an effect of the contrast in the hydrogen index between the formation and the water in the gap? For the latter effect, we considered two (water-filled) porosity conditions, 0-pu and 30-pu.

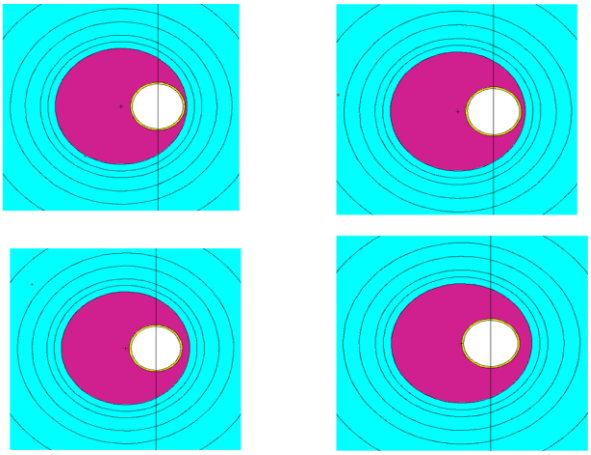

Figure 21. Water standoff of 1/8 inch, ¼ inch, ½ inch and ¾ inch, respectively.

Figure 22 displays the Det 2/Det 4 ratio of the total counts vs. standoff for the 0-pu formation.

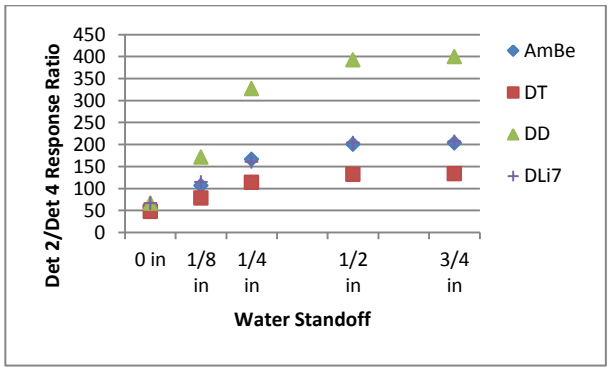

Figure 22. Standoff effect on Det 2/Det4 total counts ratio for 0-pu SiO_2 formation in the configuration of **Figure 16**.

It can be seen in **Figure 22** that, the ratio increases considerably as the standoff thickness increases for all four neutron source types. This indicates that each source will see higher 'apparent' porosity. As before, the D-D source neutrons showed the largest increase among the four source types and D-T neutrons the smallest change. We also note that as the standoff increases, the ratio begins to reach an asymptotic value, thereby answering the first posed question in the affirmative. Indeed, the ratio will depend on the standoff thickness.

Figure 23 displays the Det 2/Det 4 ratio of the total counts vs. standoff for the 30-pu formation.

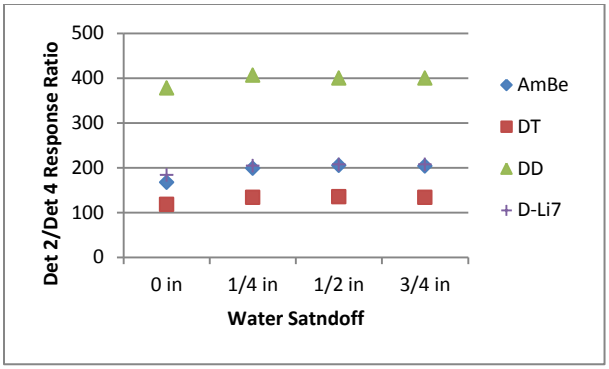

Figure 23. Standoff effect on Det 2/Det4 total-ratio porosity in 30-pu water-filled SiO_2 formation in the configuration of **Figure 16**.

The figure also shows that in the higher porosity formation, the effect of standoff, as it increases, will be much smaller relative to what was observed for the 0-pu condition. This answers the second question in the affirmative, namely, there indeed is a hydrogen index contrast effect on the standoff. Thus, the standoff effect on the computed porosity will be porosity-dependent, making it complicated to correct for.

We next compute the apparent porosity as the standoff increases. To do this, the no-standoff Det 2/Det 4 ratio in **Figure 17** was utilized as the calibration.

Figure 24 displays the apparent porosity with the 0-pu formation. Note the large overestimation of the apparent porosity from all sources, with D-T generally being the highest. At ¼ inch standoff, a 0-pu formation would look like a 28-pu formation to both Am-Be and D-T neutrons and a 19-pu formation to both D-D and D-Li7 neutrons

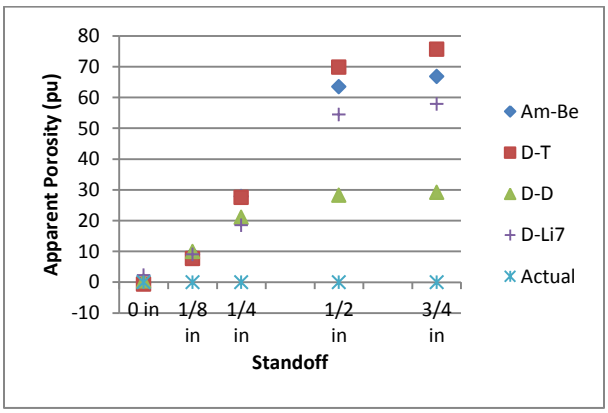

Figure 24. Apparent porosity vs. water standoff in a 0-pu SiO_2 formation.

It is also noted from **Figure 24** that as the standoff thickness increases, the differences between Am-Be and D-T, and that between D-D and D-Li7 also grow. At ¾ inch standoff, the neutron porosity is overestimated by 35 pu with Am-Be neutrons and by 45 pu with D-T neutrons.

Figure 25 displays the apparent porosity with the 30-pu formation. Again, D-T-origin neutrons exhibit the largest overestimation. At ¼-inch standoff, the over-estimation with Am-Be, D-T, D-D, and D-Li7 neutrons was about 31 pu, 46 pu, 1 pu, and 25 pu, respectively.

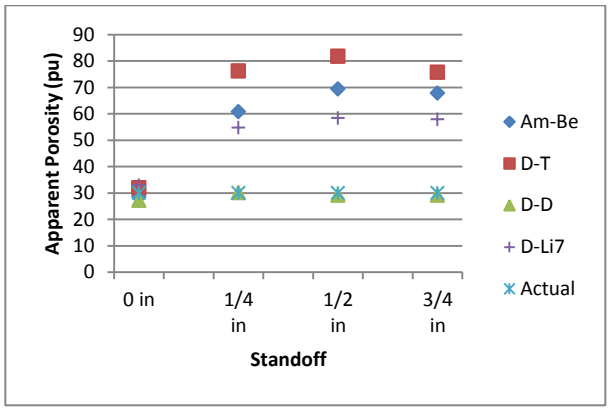

Figure 25. Apparent porosity vs. water standoff in a 30-pu water-saturated SiO_2 formation.

It is well known that epithermal neutrons are more sensitive to water standoff. This was reflected when the epithermal-ratio apparent porosity was compared to the total-ratio apparent porosity. For example, it was noted that at ¾ inch standoff, the 30-pu porosity will be over-estimated by 38-pu using Am-Be neutrons and by over 86-pu using D-T-based epithermal neutrons. This likely explains the effect seen in the field example cited in **Figure A-1** with the standoff varying as the tool goes in and out of contact with the borehole wall.

The greater overestimation with D-T neutrons arises from the fact that neutrons from this source would have a larger epithermal fraction in its total counts than other sources. While the D-Li7 neutrons have a 13.3 MeV peak, the effect is not seen because the spectrum at lower energy likely dominates the contribution to response behavior.

In both **Figure 24** and **Figure 25,** we saw that D-D neutrons result in the lowest porosity error with water stand-off despite the greater sensitivity in the Near/Far ratio. D-D neutrons become more thermalized than those from other sources. Also, as discussed previously in the paper, the 'error' is relative to a calibration condition. In this case, it is the Near/Far ratio shown in **Figure 17**. The D-D neutron-based Near/Far ratio with

standoff changes the least relative to the calibration and, thus, the error in the predicted porosity is the smallest.

Comments on Shale, Gas and Mud Effects: In this paper we confined our remarks to a water-filled formation. A more complete analysis should comment on the impact of shale, gas and possible impact of various muds used. However, the behavior of slowing down and migration lengths observed in the paper can offer some insight. For example, due to the presence of hydrogen in some shales (for example, Kaolinite), D-T neutrons will exhibit a higher impact in such shales vs. those without hydrogen (for example, Plagioclase). Whether total flux ratios or epithermal flux ratios are used for porosity will add another layer of complexity. The behavior in gas is expected to be similar but the gas density variation due to pressure variation could result in a complicated response. In addition, if the mud has a high hydrogen index or if it can absorb gas and then invade the formation, the effect can be complex, and the level of complexity will likely be different in LWD tools vs. wireline tools. [Badruzzaman et al 2005]

CHRACTERISTICS OF NEUTRON SOURCES STUDIED

This paper studied the porosity sensitivity of four neutron generators, α-Be (DPF), D-T, D-D, and D-Li7, relative to that of Am-Be source neurons. Details of the sources and their emission physics are described in **Appendix C.** For the D-T reaction, the cross-section for neutron production is the highest and, consequently, the operating voltage to achieve neutron yield is the lowest. D-T generators are already used in well logging as has been cited in the references, especially for cased-hole logging. More recently, D-T generators have been used in two wireline open-hole (n-gamma) spectroscopy tools, and in two open-hole neutron porosity tools, one for wireline logging and the other for LWD. However, due to concerns with presence of tritium which is radioactive, D-D and D-Li7 sources have been of some interest. D-D sources may offer certain response advantages relative to D-T sources. In the following sub-section, a number of source properties are considered that would directly impact use of these generators in logging tools.

Neutron yield and Logging Speed: A typical Am-Be source in a neutron porosity tool would emit about 2-4 x 10^7 neutrons per second (n/s). As the neutron yield increases, the statistical precision of the acquired counts data also improves, thereby allowing an adequate logging speed. In open-hole wireline logging, a typical logging speed is 1800 ft./hr. Clearly, a replacement-quality generator-based neutron porosity tool must be able to deliver a neutron yield in this ballpark. **Table 1** lists the nominal neutron yields of conventional neutron sources studied in this paper.

Table 1. Typical yields from different neutron sources.

Neutron Source	Nominal Yield (n/s)
Am-Be Source	2-4 x 10^7
D-T Generator	1 x 10^8
D-D Generator	1 x 10^6
D-Li7 Generator	1 x 10^6
α-Be (DPF) Generator[a]	1 x 10^7

[a]Estimated based on kinematic modeling.

From **Table 1**, we note that the DPF generator, in theory, will be able to supply a source neutron output of the same order of magnitude as that of Am-Be logging source. The D-T neutron yield is considerably higher. Thus, well logging tools equipped with D-T generators will definitely achieve the conventional logging speed and may allow a faster logging speed for the same precision. In fact, Radtke et al (2012) reported an (n-gamma) spectroscopy tool that utilizes a D-T generator with the neutron yield of 3x10^8 (or higher) and a logging speed of 3600 ft/hr.

With an order of magnitude lower neutron yield, conventional D-D and D-Li7[3] generators would demand stationary measurements in view of the inverse of square root rule, with the standard deviation varying ~ $1/\sqrt{N}$, where N represents the counts. Thus, from a source-yield perspective, currently available D-D and D-Li7 generators are unlikely to deliver typical logging speeds.

Operating at higher power (voltage x current) can increase the neutron yield of a generator. **Table 2** displays the power and voltage required to yield 2 x 10^7 n/s.

Clearly, currently available compact D-D and D-Li7 generators would require at least one-to-two orders of magnitude greater beam power to achieve neutron yields comparable to that from an Am-Be logging tool

[3] Coventry and Jurczyk (2016) showed that in a thick target, the neutron yield of D-Li7 generators would be lower than that shown for D-D generators.

source. The DPF accelerator is at an early stage of research and thus such a value was not available.[4]

Table 2. Beam Power (watts) required by the generators studied in the paper to produce 2 x10^7 n/s.[5]

Incident Particle Energy (keV)	Generator Beam Power (W)		
	D-T	D-D	D-Li7
100	0.03	8	1
150	0.02	5	1
200	0.02	4	1

In studying the response characteristics of neutrons from the different sources, it was found that the greater porosity sensitivity of D-D neutrons, reflected through the Near/Far counts ratio, came from the lower Far detector counts. Thus, there will be an inherently lower precision from using D-D neutrons which may adversely impact the logging speed, even with the same neutron yield an assumption inherent in our simulation.[6] The low neutron yield of currently available D-D generators would further compound the problem.

As commented elsewhere in the paper, the counts and hence the precision of far counts of a D-D tool can be improved by moving the detector closer to the source. However, that will reduce the ratio-based porosity-sensitivity and reduce the depth-of-investigation of the detector.

Appropriately focusing the neutrons out of a generator, one can possibly extract more information from a formation. However, the actual magnitude of the differences would depend on the tool design. In addition, this design feature will face its own challenge such as correctly aligning the tool in the well-bore.

In addition to the limitations of generators noted in this section, some of the generators face other challenges. For D-T, it is the use of tritium which is a radioactive material. D-D generators are commercially available, but new development is needed to increase the neutron yield. The DPF is in early laboratory test/proof-of-concept phase though considerable progress has been made. [Povilus et al 2016] For D-Li7 neutron generators, neutron yields are also relatively low and lithium is a 'soft' material with low a melting point, making it less than an ideal target material.

OTHER LOGGING MEASUREMENTS USING NEUTRON GENERATORS

As cited in the references, open-hole (n-gamma) capture spectroscopy tools using Am-Be sources were first reported in the 1990's. [Herron and Herron 1996] The spectroscopy data provided a mineralogical description of the geology, but since only capture-induced gamma rays are used, one cannot delineate key elements such as carbon, aluminum, magnesium, etc. For example, carbon is critically important in quantifying organic carbon content, magnesium helps differentiate limestone ($CaCO_3$) from dolomite ($CaCO_3MgCO_3$), and aluminum helps quantify clay content directly.

As noted in the references, D-T generator-based (n-gamma) spectroscopy tools, supplying gamma-rays from both inelastic and capture interactions, were recently developed to obtain a more complete mineralogical characterization of the formation. [Pemper et al 2006; Radtke et al 2012] Such tools were recently shown to allow assessment of a complex reservoir that other logging techniques, non-nuclear or radionuclide-based, could not fully resolve. [Chatterjee et al 2016] Inelastic reactions help identify carbon, magnesium, and aluminum directly from measured data, in addition to such elements as sodium, sulfur, etc., which are critical in assessing unconventional reservoirs. D-D neutrons, at 2.45 MeV, are below inelastic scattering thresholds such as, for example, the carbon gamma-rays emitted at 4.44 MeV. Measuring the carbon signal in conjunction with identifying elements such as magnesium, sodium, etc., is essential in differentiating organic carbon (which is from hydrocarbons) from inorganic carbons i.e., those in the rock itself such as that in limestone ($CaCO_3$), nahcolite ($NaHCO_3$), etc.

As noted elsewhere in the paper, an appropriately designed D-T generator tool can also supply a formation density (the so-called INGD) albeit, a less accurate one.

[4] T-T neutron generators have also been of interest due to the similarity of their neutron spectrum to the Am-Be spectrum. However, their low neutron yield (2 x 10^6 n/s) and the added tritium make them unattractive as source of neutrons in a well logging tool.

[5] D-T, and D-D yields derived from Shope LA, "Theoretical Thick Target Yields for the D-D, D-T, and T-D Nuclear Reactions Using the Metal Occluders Ti and Er and Energies up to 300 keV," Report SC-TM-66-247, Sandia National Laboratories, Albuquerque, N.M. (1966). D-Li7 yields derived from Chichester, D.L., "Production and Applications of Neutrons Using Particle Accelerators", Idaho National Laboratory Report INL/EXT-09-17312, November, 2009.

[6] In our simulation we assumed a unit source i.e., the same neutron yield from all sources.

D-D neutrons are able to provide gamma rays for (n-gamma) capture spectroscopy. However, D-D neutron sources will not be able to identify carbon, aluminum, magnesium sodium, etc. by this technique. In addition, since at a given logging speed, the statistical precision in estimating elemental concentrations will be poorer than that achieved for bulk parameters such as porosity and density, the logging speed even in (n-gamma) capture measurements would likely be considerably lower. We had noted previously in the paper that the neutron yield of currently available compact, low-power D-D generators will likely not suffice for the bulk parameters. Clearly, it will be even more problematic in spectroscopy measurements.

In addition to producing a lower energy neutron spectrum similar to that from an Am-Be source, a D-Li7 neutron generator produces neutrons at 13.3 MeV, offering the potential for obtaining some of the inelastic interaction-based parameters that D-T generator tools currently provide. However, due to the low neutron yield of a D-Li7 generator, it is unlikely to produce a sufficient number of gamma rays from inelastic scattering. If the neutron yield can be increased to the level for D-T generators, one may be able get (n-gamma) inelastic spectra of sufficient precision. However, issues in developing robust targets for high output neutron generators would likely arise.

SUMMARY

This paper examined the potential of four types of neutron generators, α-Be (DPF), D-T, D-D, and D-Li7, to replace the Am-Be source in neutron porosity tools. The study was conducted primarily from the perspective of interpretation and data quality and, secondarily, to understand the state of generator hardware as it impacts the interpretation.

We examined both nominal and more complex conditions such as low porosity, the presence of strong thermal absorbers, and tool standoff. The data quality determines the logging speed, a key operational parameter. In addition, we briefly commented on the prospect of replacing Am-Be-based (n-gamma) spectroscopy tools using generator-based neutrons. We draw the following conclusions from the study.

- If successfully developed, α-Be (DPF) generators could provide a direct replacement of Am-Be sources with a compact source of neutrons. However, they are still in early research phase. Their (n-gamma) spectroscopy capability in well logging would likely to be similar to that of Am-Be tools, namely, be limited to (n-gamma) capture spectroscopy.

- The analysis shows that D-D generator neutrons offer the largest porosity sensitivity of the neutron sources studied and would be least affected by tool standoff. We also found that D-D neutrons may even provide better resolution of the porosity in the low-porosity range.

- The response of D-Li7 source would be similar to that from Am-Be source neutrons. The standoff effect would be considerably lower than that of D-T neutrons. The low-porosity sensitivity would be better than that of Am-Be or D-T neutrons.

- The effect of thermal absorbers would be substantial for all neutron sources.

- Both D-D and D-Li7 generators are tritium-free while the tritium content of D-T generators can be substantial.

- The greater porosity sensitivity of D-D neutrons comes at the expense of lower neutron counts at the Far detector. This would degrade the precision and reduce the logging speed, even if the neutron yield were the same as that of D-T generators. The low neutron yield of D-D generators would further compound the problem and only stationary measurements may be feasible with currently available D-D sources.

- Similarly, the low neutron yield of D-Li7 generators would likely only allow stationary measurements. The challenges with lithium as a target also need to be addressed.

- The neutron yield of D-T generators under nominal conditions (100 keV) is about an order of magnitude higher that the Am-Be logging source and two orders of magnitude higher than that from conventional D-D or D-Li7 generators. Thus, the logging speed of D-T tools would be compatible with induction and acoustic tools. In fact, one may be able utilize higher logging speed with a D-T tool, as cited from the work of Radtke et al (2012).

- One way to increase the neutron yield from D-D or D-Li7 generators is by using higher beam power. Relative to D-T generators, the power will have to be boosted significantly; for example, a factor of 200 for D-D generators and 1450-fold for D-Li7 generators at 200 keV. Another way to increase the neutron yield would be to develop more

efficient ion sources that produce higher fractions of monatomic ions in the beam. In either case, considerable hardware R&D would be required.

- D-T generator-based porosity tools exhibit lower porosity sensitivity vs. the other generators studied. This in turn results in a larger effect from presence of absorbers and from tool standoff. The lower porosity sensitivity can possibly be overcome, in many conditions, with design changes, but that may make the tool more complicated to utilize in complex wellbores. One example of such a design change in a D-T LWD tool was reported by Xu et al (2010) where the authors were able to achieve an Am-Be-like porosity by placing the Far detector farther away. The drawback is that this makes the tool longer and more difficult to deploy in holes with twists and turns. In addition, the technique may not work for wireline tools or in all well-bore conditions since the physics of D-T neutrons and their transport will be different in wireline versus LWD applications.

- Due to the low energy of source neutrons, D-D generator-based tools will not be able to supply the parameters that can now be obtained from inelastic (n-gamma) spectroscopy using D-T neutrons which provide a more complete mineralogy. D-D generator tools, in principle, can supply (n-gamma) capture spectroscopy information, but their low neutron yield may not provide sufficiently resolved spectral data.

- Due to neutrons also being emitted at 13.3 MeV by D-Li7 generators, it should be possible, in principle, to obtain inelastic (n-gamma) spectroscopy-based parameters. However, as in the case of D-D generators, the low neutron yield from D-Li7 generators would likely allow only stationary porosity measurements. The situation would be worse for (n-gamma) spectroscopy.

- Despite their limitations, D-T neutron generators offer the potential for utilizing a single device to obtain multiple petrophysical parameters, such as neutron porosity, bulk lithology, clay content, mineralogy to quantify organic versus inorganic carbon content, etc., resulting in a more complete characterization of the formation. An appropriately designed D-T tool can even provide a pseudo-density (i.e., "poor-man's density") in case Cs-137 sources cannot be used for density. In fact, such a multiple-parameter tool has been marketed for LWD applications as noted previously in the paper and described in the references, Evans et al (2000) and Reichel et al (2012).

Our analysis confirms what is generally well-known in the industry, namely, that replacing Am-Be sources tools for neutron porosity will be complicated. [Gilchrist et al 2011] Only the DPF accelerator is expected to be a direct replacement of Am-Be sources since it produces a nearly identical source-neutron spectrum. Its development is at an early stage and many questions regarding its applicability in harsh logging conditions and power requirements will have to be addressed before logging tools can be designed with a DPF accelerator. Additionally, its spectroscopy repertoire would be limited relative to a D-T based tool.

Each of the generators face several technical challenges as summarized above. It is unlikely that a single generator concept would meet all requirements. If both Am-Be-like neutron porosity and D-T generator-like spectroscopy are desired, perhaps a DPF-based tool, if perfected, could replace the Am-Be source while D-T tools can be used in (n-gamma) spectroscopy only. On the other hand, a combination of an enhanced generation D-D porosity tool with a D-T tool for spectroscopy can provide a better-quality neutron porosity with a more complete mineralogy. Of course, one will have to contend with legacy data issues.

Finally, if the simplicity of a single, multiple-parameter tool is desired, a D-T generator wireline tool similar to its LWD version, with both neutron and gamma detectors incorporated, is perhaps the choice. Development of such a tool would require that the neutron porosity from the tool can be corrected sufficiently, for example for standoff, with design and appropriate physics-based algorithms. Here too legacy data issues have to be resolved. The petroleum industry already has considerable experience with D-T generator tools starting with decades of use in cased-hole logging tools, in (n-gamma) spectroscopy tools, and recently in the multi-parameter LWD tool reported by Evans et al (2000) and. Reichel et al (2012). Whether a multi-parameter tool can be replicated for wireline logging applications, with acceptable quality, should perhaps be explored.

ACKNOWLEDGEMENTS

Sandia National Laboratories is a multi-mission laboratory managed and operated by National Technology and Engineering Solutions of Sandia, LLC., a wholly owned subsidiary of Honeywell International, Inc., for the U.S. Department of Energy's National Nuclear Security Administration under

contract DE-NA0003525. Prepared in part by LLNL under Contract DE-AC52-07NA27344 and supported by US DOE/NA-22 Office of Non-proliferation Research and Development.

REFERENCES

Badruzzaman A, 1998, Multidetector Pulsed-Neutron Through-tubing Cased-Hole Density Measurement Sonde, U.S. Patent No. 5,825,024.

Badruzzaman A, 2005, Nuclear Logging Technology, Present and Future-An Operating Company Perspective, Petrophysics, **46**, No. 3, 220-236.

Badruzzaman A, Adeyemo AO, Logan Jr. JP, Sheffield J, Stonard SW, 2005, The ubiquitous neutron/density tool response in petro-free mud: *New insights to addressing unresolved issues?* Proc. 46th SPWLA Annual Symposium, New Orleans, June 26-29. Paper KK

Badruzzaman A, Barnes S, Bair F, and Grice K, 2009, Radioactive Sources in Petroleum Industry: Applications, Concerns and Alternatives, Paper SPE-123593, presented at the SPE Asia Pacific Health, Safety, Security, and Environment Conference and Exhibition, Jakarta, Indonesia, 4-6 August.

Badruzzaman A, 2014, An Assessment of Fundamentals of Nuclear-based Alternatives to Conventional Chemical Source Bulk Density Measurement, Petrophysics, **55**, 5, 415-434.

Bosch, H.S. and Hale, G.M., 1992, Improved Formulas for Fusion Cross-Sections and Thermal Reactivities, Nuclear Fusion, **32**, 4, 611-631.

Chatterjee A, Baig MH, Sylta K-EH, Datir H, Donadille J-M, Leech R, Kollien T, Foyn SE Gianotten IP, 2016, The Conglomerates Challenge: Evaluating The New Hydrocarbon Plays on the Norwegian Shelf, Trans. 57th SPWLA Annual Symposium, Paper A.

Chen AX, Antolak AJ, Leung, K-N, 2012, Electronic neutron sources for compensated porosity well logging, Nuclear Instruments and Methods in Physics Research A, 684, 52–56.

Chichester, D.L., "Production and Applications of Neutrons Using Particle Accelerators", Idaho National Laboratory Report INL/EXT-09-17312, November, 2009.

Coventry DM and Jurczyk BE, 2016, "Development of Neutron Generators to Replace AmBe Radionuclide Neutron Source in Oil/Gas Applications," Proc. 2016 INMM Conference, Atlanta, GA.

Ellis DV, 1987, Well Logging for Earth Scientists, Elsevier, New York

Ellis DV and Singer JM, 2007, Well Logging for Earth Scientists, Second Edition, Springer, New York.

Evans M, Adolph R, Vilde L, Morris C, Fissler P, Sloan W, Grau J, Liberman A, Zeigler W, Loomis WA, Yonezawa T, Sugimura Y, Seki H, Misawa RM, Holenka J, Borkowski N, Dasgupta T, and Borkowski D, 2000, "A sourceless alternative to conventional LWD nuclear logging," SPE 62982, in Proc. SPE Annual Technical Conference and Exhibition, Dallas, TX, 3-4 October.

Flanagan WD, Bramblett RL, Galford JE, Hertzog RC, Plasek RE, and Oleson JR, 1991, "A New Generation Nuclear Logging System," in Proc. SPWLA 32nd Annual Logging Symposium, Midland, TX. June, 16-19. Paper Y.

Fricke S, Madio DP, Adolph B, Evans M, Leveridge R, 2008, "Thermal Neutron Porosity using Pulsed Neutron Measurements," in Trans. SPWLA 49th Annual Symposium, Edinburgh, Scotland, May25-28, Paper L

Galford J, Truax J, Hrametz A, and Hatmboure C, 2009 A new neutron-induced gamma ray spectroscopy tool for geochemical logging, Trans. 50th SPWLA Annual Logging Symposium, 21-24 June, 2009, The Woodlands, TX. Paper X. Also see SPE 123992, 2008, by the same authors.

Gilchrist Jr. W.A., Inanc F, and Roberts L, 2011, "Nuclear Source Replacement – Promises and Pitfalls." In Proc. SPWLA 52nd Annual Logging Symposium, May 14-18. Paper KKK.

Guardian, 2003, "Radioactive material missing," http://www.guardian.co.uk/international/story/0,3604,902981,00.html, February 26.

Herron SL and Herron MH, 1996, Quantitative Lithology: An Application for Open- and Cased-hole Spectroscopy, in Trans. SPWLA 37th Annual Logging Symposium, Paper E.

King III, G., Bramblett, R.L, Becker, A.J., Corris, G.W., and Boyce, J.R., 1987, "Density Logging Using An Electron Linear Accelerator as the X-Ray Source,"

Nuclear Instruments and Methods in Physics Research B24/25, 990-994.

Lamarsh 1972, Introduction to Nuclear Reactor Theory, Addison-Wesley Publishing Company, Menlo Park, CA

LANL, 2003/2008, "A General Monte Carlo N-Particle Transport Code, Version 5, LA-UR-03-1987, Los Alamos National Laboratory, Los Alamos, NM. Published on April 24, 2003 and revised February 1, 2008.

Mills WR., Allen LL, and Stromswold, DC, 1988, "Pulsed neutron porosity logging based on epithermal neutron die-away," Nuclear Geophysics, 2, No. 2, p81-83, (1988).

NAS 2008, Radiation Source Use and Replacement, A report by the Committee on Radiation Source Use and Replacement of Nuclear and Radiation Studies Board, Division on Earth and Life Studies, National Research Council, US National Academy of Sciences, Wash. DC.

Neuman CH, Sullivan MJ, and Belanger DL, 1999, "An Investigation of Density Derived from Pulsed Neutron Capture Measurements," SPE 56647, in Proc. of SPE Annual Technical Conference and Exhibition, Houston, TX., 3-6 October.

NRC 2006, "AGREEMENT STATE REPORT - WELL LOGGING SOURCE DAMAGED," Event Number: 42891, CA Report Number: 100706, a report from State of California to US Nuclear Regulatory Commission, October 8.

Odom RC, Streeter RW, Wilson RD, 1999, Formation density measurements utilizing pulse neutrons, US Patent 5,900,627, April 4.

Pemper R, Sommer A, Guo P, Jacobi D, Longo, J, Bliven S, Rodriguez E, Mendez F, and Han X, 2006, A new pulsed neutron sonde for derivation of formation lithology and mineralogy, SPE 102770, In: Proc. SPE Annual Technical Conference and Exhibition 24-27 September.

Povilus A, Crank M, Falabella S, Higginson D, Jiang S, Link A, Shaw, B, and Schmidt A, 2016, "AmBe Source Replacement via Dense Plasma Focus Z-Pinch," Proc. INMM Proc. 2016 INMM Conference, Atlanta, GA.

Radtke RJ, Lorente M, Adolph B, Berheide M, Fricke S, Grau J, Herron S, Horkowitz J, Jorion B, Madio D, May D, Miles J, Perkins L, Phillip O, Roscoe B, Rose D, Stoller C, 2012, A New Capture and Inelastic Spectroscopy Tool Takes Geochemical Logging to Next Level, In: Proc. 53rd SPWLA Annual Symposium, Cartagena, Columbia, June 16-20.

Reichel N, Evans M, Allioli F, Mauborgne M-L, Nicoletti L, Haranger F, Laporte N, Stoller C, Cretoiu V, Hehiawy E. El, and Rabrei R, 2012, "Neutron-Gamma Density (NGD): Principles, Field Test Results and Log Quality Control of a Radioisotope-free Bulk Density Measurement," in Proc. SPWLA 53rd Annual Symposium, Cartagena, Colombia, June 16-20. Paper GGG.

Rhodes W, 2010, "The RDD Threat and the Global Threat Reduction Initiative's (GTRI) Domestic Security Efforts," presented at the PNNL Workshop on *Alternatives to Chemical Radiation Sources for Petrochemical Well Logging*, University of Houston, October 27-28.

Schmidt A, Tang V, and Welch D, 2012, "Fully Kinetic Simulations of Dense Plasma Focus Z-Pinch Devices," Physical Review Letters, 109(20): p. 205003.

Scott HD, Wright PD, Thornton JL., Olsen J-R., Hertzog RC, McKeon DasGupta T, and Albertin IJ, 1994, "Response of a multidetector pulsed neutron porosity tool," paper J, in 35th Annual Logging Symposium Transactions: Society of Professional Well Log Analysts.

Shope LA, 1966, "Theoretical Thick Target Yields for the D-D, D-T, and T-D Nuclear Reactions Using the Metal Occluders Ti and Er and Energies up to 300 keV," Report SC-TM-66-247, Sandia National Laboratories, Albuquerque, N.M.

Valant-Spaight B, Han W, Guo W, and Schultz W, 2006 "Field Examples with a Slim LWD Density/Neutron Instrument Containing a Californium-252 Neutron Source and Three Neutron Detectors," in Proc. 47th SPWLA Annual Logging Symposium. Paper CCC.

Wilson RD, 1995, "Bulk Density Logging with High-Energy Gammas Produced by Fast Neutron Reactions With Formation Oxygen Atoms," Paper NSS11-01, Trans. IEEE Nuclear Science Symposium, San Francisco, CA, October 21-28.

Xu L, Schultz W, Huiszoon C, 2010, "A Comprehensive Investigation of Source Effects on Neutron Porosity Response for Logging-While-Drilling Measurements, Petrophysics," Vol. 51, No. 3, p185-198, June.

ABOUT THE AUTHORS

Ahmed Badruzzaman studied downhole nuclear techniques during his 37 years of R&D tenure at Chevron, Sandia National Laboratories, and Schlumberger-Doll, and teaching at UC Berkeley. His current research is on advanced nuclear logging concepts. An SME consultant to the US Department of Energy (DOE) on mitigating security/safety risks of radionuclide-based well logging tools and assessing alternative technologies, he led DOE's 2015 scoping study on the latter. Ahmed has been a primary industry discussant on the topic through his papers, a patent on the inelastic (n-gamma) density technique, and leadership of SPWLA's Nuclear Logging SIG. He was a consultant to the IAEA and Vienna-based WINS on source issues, and an official reviewer of US National Academy Sciences' 2008 report to Congress on industrial sources. Author of over 40 papers, two US patents, and an upcoming textbook on Nuclear Logging, Ahmed is a Fellow of American Nuclear Society, a two-time SPWLA Distinguished Speaker, a former SPE Distinguished Lecturer, and winner of several technical awards. In addition to continuing research on nuclear logging techniques, Ahmed is now engaged in two teaching activities, namely, offering PetroSkill's Cased Hole FE course, and co-teaching UC Berkeley's Big Ideas course, *Energy and Civilization*. He holds a PhD in Nuclear Engineering & Science from Rensselaer Polytechnic Institute, Troy, NY. He can be reached at ahmed.badruzzaman@gmail.com

Andrea Schmidt received her B.A. in Physics from the University of California, Berkeley, in 2004, and her Ph.D. in Physics from MIT in 2011. She joined LLNL as a postdoctoral researcher in 2011 and then joined the staff in 2013. As a postdoc, she performed the first kinetic modeling of a short-pulse neutron source called a dense plasma focus (DPF), demonstrating that a particle approach was needed to correctly capture beam formation and neutron yield. She is now leading several neutron source development projects that have both modeling and experimental components. She has been developing neutron sources for 6 years and working with fusion plasmas for 7 additional years prior. She is also a group leader for Engineering's Plasma Engineering group and an APL in the Physics' directorate Pulsed Power Fusion Plasmas group.

Arlyn Antolak in the DHS & Defense Systems Center, Sandia National Laboratories, Livermore, CA has led a variety of research and technology development projects in accelerators, radiation transport, materials science, and nuclear physics. He has over 70 technical publications in the areas of nuclear, atomic, solid state physics, and materials science. He has led particle accelerator R&D at Sandia in particular developing compact, low-power sources using low-energy nuclear reactions to produce high-energy emission particles for active interrogation (compact dual-particle neutron/gamma source), well logging (gamma source to replace Cs137), and nonproliferation (negative ion-driven neutron generator). His work has been recognized with national awards including the R&D100 Award and a US-DOE Defense Programs Award of Excellence, as well as several Sandia employee recognition awards. He has an MS in Nuclear Engineering and PhD in Applied Physics from Northwestern University, Evanston, IL.

APPENDIX A. EXAMPLE OF POROSITY FROM A D-T GENERATOR NEUTRON POROSITY TOOL

The following is an example from one of the references that illustrated interpretation challenges that may arise from switching sources of neutron tools. [Badruzzaman 2005] The tool, using epithermal neutrons, was run in a high-temperature, high-pressure (HTHP) sandstone reservoir.

Figure A-1 (Track 2) illustrates the spiky behavior of the neutron porosity seen in a number of wells in clean sandstone zones.

The cause of the spikes in the neutron porosity was not clear. The conjecture was that there were operations, design, and physics issues. From the results in this paper, it appears that the likely cause was variable standoff due to loss of continuous contact with the wellbore wall. Such loss of contact may arise if the bow-spring to push the tool up against the borehole wall is not properly placed or is not used. Use of the porosity displayed in **Figure A-1** would result in predicting the clearly clean sandstone as limey dolomite.

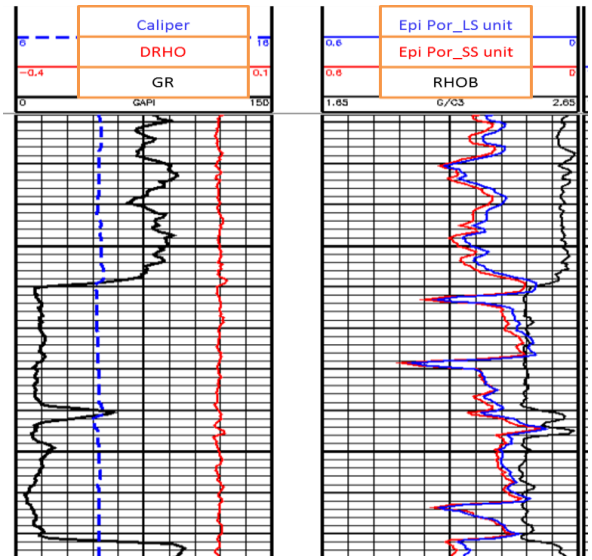

Figure A-1. Porosity from an epithermal porosity tool in wet sandstone. The epithermal porosity (Epi Por) is depicted in Track 2. LS and SS stand for limestone and sandstone, respectively. The meanings of the other parameters in the figure are standard.

APPENDIX B: NEUTRON SLOWING DOWN MIGRATION, AND DIFFUSION LENGTHS

In spherical geometry we assumed, we can use the analytical solution of the diffusion equation to cast the N/F epithermal ratio as follows (Ellis 1987):

$$R_{N/F}^{Epi} = \frac{\varphi_1(r_N)}{\varphi_1(r_F)} = \frac{r_F}{r_N}\exp\left[-(r_N - r_F)/L_s\right], \quad \text{(B-1)},$$

where φ_1 denotes the group 1 (or epithermal) flux in a two-energy-group (epithermal and thermal) model, and r_F and r_N are far and near locations, respectively.

Using an approximation procedure borrowed from reactor physics (Lamarsh 1972) that further simplifies the two-energy-group model, we can utilize the N/F ratio of total flux in an equation similar to Eq. (B-1) where we replace the slowing down length L_s by a parameter, L_m, we term as the migration length. L_m is defined by

$$L_m^2 = L_s^2 + L_d^2, \quad \text{(B-2)}$$

where L_d is denoted as the diffusion length. L_d is defined using the diffusion coefficient of thermal neutrons and their absorption cross section, $\boldsymbol{\Sigma}$, as follows.

$$L_d^2 = \frac{D_{Th}}{\Sigma}. \quad \text{(B-3)}$$

L_d can also be obtained using diffusion theory but the procedure is more complex.

APPENDIX C. NEUTRON GENERATORS: BASICS AND HARDWARE STATUS

Am-Be Neutrons: Americium 241 is an α-emitter. Neutrons are produced from the interaction of the α-particles such as Be^9 in a mixture of the two resulting in the neutron spectrum displayed in **Figure 1** in the main body of the paper. Note that the average energy of the spectrum is a little above 4 MeV.

DPF Accelerator Neutrons: The dense plasma focus (DPF) z-pinch accelerates helium (α-particles) onto to a beryllium (Be) target to produce neutrons from the α-Be reaction, much like the Am-Be source. As shown in **Figure C-1**, it is essentially a coaxial plasma rail gun which connects the long time scale of a capacitor discharge with the short time scale of a z-pinch through inductive store of magnetic fields.

A plasma first flashes over the insulator, then runs down the gun, propelled by its self-generated magnetic field. When the plasma reaches the end of the gun, it runs in and pinches, accelerating an energetic ion beam.

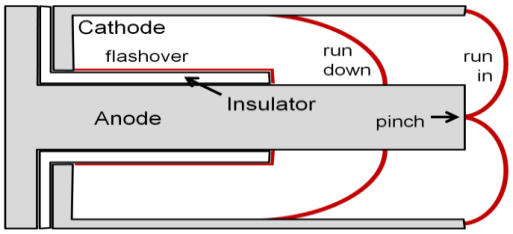

Figure C-1. Schematic of a dense plasma focus (DPF).

Through an increase in plasma resistivity during the z-pinch phase, DPFs can accelerate an ion beam with energies up to several MeV. Thus, a compact device operated at only 25 kV can produce multiple MeV ions. The spectra displayed in **Figure 1** in the main body of the paper were obtained from calculations using first principles kinematics and measured cross-sections of both DPF and Am-Be.

The DPF is likely the only compact accelerator technology that may be able reproduce the Am-Be spectrum through acceleration of helium ions (α particles) into a beryllium target. This is because the α-Be cross-section is negligible below ~2 MeV. Conventional accelerator technology would be far too bulky to accelerate helium to 2 MeV within the size

constraints of a bore-hole. There are nuclear reactions that could be used which produce >2 MeV helium ions as one of their products. For example, the D-T reaction produces a 14 MeV neutron and a 3.5 MeV alpha particle. A further discussion of this is beyond the scope of the paper.

D-T, D-D, and D-Li7 Neutrons: These neutrons are produced from well-known nuclear and fusion reactions. In the D-T reaction, deuterium is accelerated onto a tritium target to produce 14.1 MeV neutrons and α-particles. In the D-D reaction, deuterium is accelerated onto a deuterium target producing 2.45 MeV neutrons and He^3 ions 50% of the time, and 1.01 MeV tritium ions and 3.02 MeV protons the other 50% of the time. In the D-Li7 reaction, deuterium is accelerated onto to a lithium-7 target producing beryllium-9 and neutrons with the spectrum depicted in **Figure 2** in main body of the text of the paper plus high energy neutrons at 13.3 MeV. The reaction also produces gamma rays at 12, 14, 15 and 17 MeV.

Table C-1 lists the cross-section of these interactions at various operating voltages, and beam powers. Note that the cross-section (probability of interaction) of the D-T reaction is much higher than those of the other two reactions. Note that the maximum of the D-T reaction cross-section is at 100 keV of the deuterium projectile energy. For the other two reactions, the operating voltage required to reach their respective higher cross section values is much higher.

Table C-1. Reaction cross sections in millibarn (mb) and beam power (Watt) as a function of operating voltage (keV) for various types of neutron generators.[a]

keV	D-T		D-D		D-Li7	
	mb	Watts	mb	Watts	mb	Watts
100	4900	0.03	18	11	0.5	540
200	2550	0.02	38	4	15	29
300	1280	0.02	55	3	50	4
600	750		80		500	

[a]100-keV and 200-keV values are from Strelnikov YV, Abramovich SN, Morkin LA, Yureva ND, Bull. Acad. Sci. USSR, Phys. Ser. 35, 149 (1972); 300-keV and 600-keV values are extrapolated

A major drawback of D-T generators is the use of several curies tritium with a half-life of 12.5 years. Leakage of tritium can be problematic. D-Li7 generators do not have tritium but the melting point of lithium is low, making it a less ideal target material. If a pure lithium target cannot be adequately developed, then more robust lithium compounds could be tested but this would be at the expense of further reduced neutron yield at a given power.

From a hardware perspective, D-D generators offer some advantages. They do not contain tritium and they are commercially available. On the other hand, most commercially available D–D neutron generators have rather low neutron yields of around 10^6 n/s at their nominal 100 keV operating voltage. The low output is due to two main factors: 1) low neutron production cross section for the D-D fusion reaction and 2) the use of an inefficient Penning discharge ion source. With a Penning source, the neutron yield is low because the production of monatomic (D^+) ions is very low (~10%). Several efforts have been underway to increase the neutron yield of D-D generators. To achieve higher neutron yields, the generator needs to operate at much higher power or a more efficient ion source is needed. Several efforts have explored field emission-type ion sources for use in extremely compact, low power and high yield D-D neutron generators. Efficient RF or microwave discharge plasmas have also demonstrated high atomic fraction ion beams for improved neutron production. A commercial RF-based D-D neutron generator is available that produces up to 5 x 10^7 n/s at its nominal 120-140 keV operating voltage.